Title

Materials Genome in Action: Identifying the Performance Limits of Physical Hydrogen Storage.

Journal

Chemistry of materials : a publication of the American Chemical Society, 29(7)

ISSN

0897-4756

Authors

Thornton, Aaron W
Simon, Cory M
Kim, Jihan
et al.

Publication Date

2017-04-01

DOI

10.1021/acs.chemmater.6b04933

Peer reviewed

CHEMISTRY OF MATERIALS

Article

pubs.acs.org/cm

Materials Genome in Action: Identifying the Performance Limits of Physical Hydrogen Storage

Aaron W. Thornton,[*,†] Cory M. Simon,[‡] Jihan Kim,[§] Ohmin Kwon,[§] Kathryn S. Deeg,[∥] Kristina Konstas,[†] Steven J. Pas,[⊥,#] Matthew R. Hill,[†,▽] David A. Winkler,[†,○,¶,◇] Maciej Haranczyk,[∞] and Berend Smit[‡,∥,&]

[†]Future Industries, Commonwealth Scientific and Industrial Research Organisation, Private Bag 10, Clayton Southth MDC, Victoria 3169, Australia

[‡]Department of Chemical and Biomolecular Engineering and [∥]Department of Chemistry, University of California, Berkeley, California 94720-1462, United States

[§]Department of Chemical and Biomolecular Engineering, Korea Advanced Institute of Science and Technology, 291 Daehak-ro Yuseong-gu, Daejeon, 305-701, Korea

[⊥]Power & Energy Systems, Maritime Division, Defence Science and Technology Group, Department of Defence, 506 Lorimer Street, Fishermans Bend, Victoria 3207, Australia

[#]School of Chemistry and [▽]Department of Chemical Engineering, Monash University, Clayton, Victoria 3800, Australia

[○]Monash Institute of Pharmaceutical Sciences, 381 Royal Parade, Parkville, Victoria 3052, Australia

[¶]Latrobe Institute for Molecular Science, Bundoora, Victoria 3046, Australia

[◇]School of Chemical and Physical Sciences, Flinders University, Bedford Park, South Australia 5042, Australia

[∞]Computational Research Division, Lawrence Berkeley National Laboratory, Berkeley, California 94720-8139, United States

[&]Laboratory of Molecular Simulation, Institut des Sciences et Ingénierie Chimiques, Valais, Rue de l'Industrie 17, Ecole Polytechnique Fédérale de Lausanne (EPFL), CH-1950 Sion, Switzerland

Supporting Information

ABSTRACT: The Materials Genome is in action: the molecular codes for millions of materials have been sequenced, predictive models have been developed, and now the challenge of hydrogen storage is targeted. Renewably generated hydrogen is an attractive transportation fuel with zero carbon emissions, but its storage remains a significant challenge. Nanoporous adsorbents have shown promising physical adsorption of hydrogen approaching targeted capacities, but the scope of studies has remained limited. Here the Nanoporous Materials Genome, containing over 850 000 materials, is analyzed with a variety of computational tools to explore the limits of hydrogen storage. Optimal features that maximize net capacity at room temperature include pore sizes of around 6 Å and void fractions of 0.1, while at cryogenic temperatures pore sizes of 10 Å and void fractions of 0.5 are optimal. Our top candidates are found to be commercially attractive as "cryo-adsorbents", with promising storage capacities at 77 K and 100 bar with 30% enhancement to 40 g/L, a promising alternative to liquefaction at 20 K and compression at 700 bar.

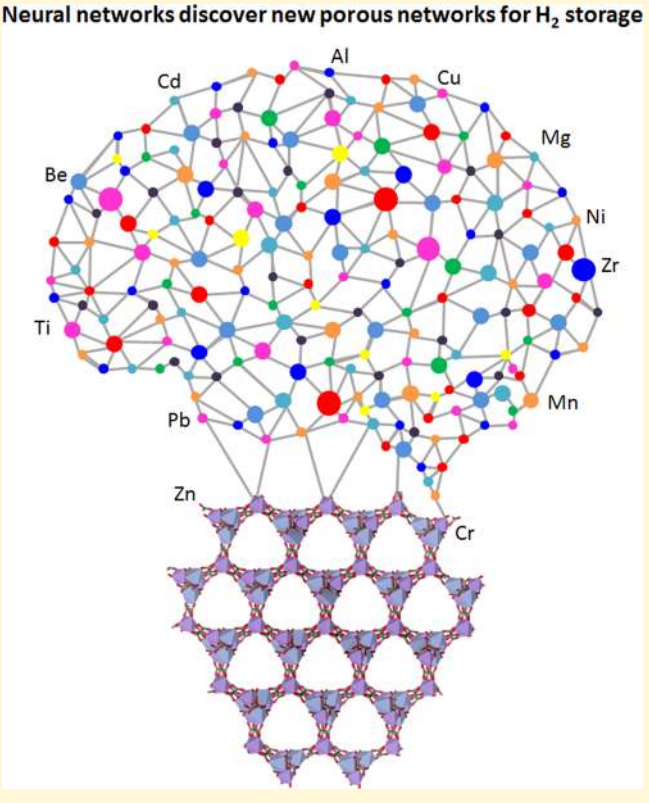

Received: November 21, 2016
Revised: March 6, 2017
Published: March 8, 2017

DOI: 10.1021/acs.chemmater.6b04933
Chem. Mater. 2017, 29, 2844−2854

1. INTRODUCTION

Hydrogen will play a role in the future composition and market share of the transportable fuels economy due to its zero carbon emissions.[1−3] The transportation sector currently accounts for ∼27% of U.S. greenhouse gas emissions.[4] There is growing interest in renewable hydrogen production, by solar-based water hydrolysis, for example. Hydrogen can be readily used as a transportable and on-demand power source that emits only pure water vapor.[5] However, a significant hurdle to adopting hydrogen technology is the storage component, which is energy intensive and suffers from low volumetric energy density—a factor of 3000 lower than that of gasoline.[6] Consequently, hydrogen is currently compressed (up to 700 bar) or liquefied (cooled to 20 K) to achieve a higher volumetric energy density. However, there are significant energy and infrastructure (capital) requirements associated with these conventional methods of storage, as well as safety concerns.

Chemisorption or physisorption of hydrogen within solid state materials provides an alternative to conventional mechanical-based approaches to densifying hydrogen. Exploiting the thermodynamic advantages of physical adsorption, we consider porous material adsorbents to achieve a high density of hydrogen that is deliverable within a moderate pressure range. Chemisorbents, on the other hand, require heat to release the hydrogen and can suffer from slow release kinetics.[7] Advanced physisorbents provide disruptive alternatives to hydrogen storage because of their tunable interactions and nanoconfined environments that can attract, capture, and release hydrogen with higher efficiency, convenience, and safety. This is particularly the case for metal−organic frameworks (MOFs), where several reviews have highlighted their steadily improving storage performance.[7−12]

Motivated by the Human Genome, the Materials Genome Initiative was set up by the White House to unify materials research, with the common aim to "discover, develop, and deploy new materials twice as fast" compared with current methods.[13,14] In the same way that simple building blocks such as amino acids can lead to proteins with diverse biological functions, combining different chemical building blocks can form materials with diverse functions. The Nanoporous Materials Genome (NMG)[15] represents a growing set of over 3 million predicted[16−20] and synthesized[21] materials contributed by a variety of research groups. This initiative has tackled problems including xenon/krypton separation,[22] production of fuels and chemical feedstocks,[23] catalytic conversion of carbon dioxide,[24] room temperature storage of hydrogen,[25] small molecule adsorption in open-site MOFs,[26] evolutionary design of materials,[27] and many mor,e[18,20,21,28−33] including the recent search for methane storage materials.[34]

Recently, Simon et al. screened the complete NMG database using a large-scale, multistep computational screening process to discover the limits of methane storage.[34] In the same spirit, this present work analyzes the NMG database to identify the limits of hydrogen storage using porous materials.

Virtual (or in silico) screening has become a powerful tool to discover promising candidate adsorbents in very large chemical or structural parameter spaces. For example, the approach has been applied to the selection of compounds that bind to proteins,[35] MOF analogues for water adsorption,[36] MOFs for fossil fuel purification,[37] zeolitic materials for carbon capture,[19,38] and porous adsorbents for the separation of linear, mono-branched, and dibranched isomers of alkynes for petrochemical separations.[39] Machine learning methods play a critical role in the large-scale search for novel materials, where multiple structural descriptors are available, and complex, nonlinear relationships are observed between the target property and the descriptors in high-dimensional feature spaces. Fernandez et al. adopted the quantitative structure−property relationships approach to identify MOFs for methane storage, which revealed the importance of pore sizes and void fraction.[40] Thornton et al. utilized machine learning to optimize the dual adsorption of hydrogen and carbon dioxide in zeolites,[24] while Simon et al. accelerated the discovery of porous materials for xenon/krypton separations based on random forests.[22] Other examples include the prediction of drug efficacy,[41] biocompatibility of polymers,[42] solubility in different solvents,[43,44] mutagenicity of chemicals,[45] carbon capture materials,[46] and bacterial attachment to polymers.[47]

This study is limited to well-defined crystalline nanoporous materials that can be considered a subset of the Materials Genome Initiative. There are amorphous structures capable of achieving high hydrogen capacity, such as activated carbons, that are also competitive on cost and availability.[48] For example, porous aromatic frameworks are amorphous despite their short-range order and have exceptional hydrogen capacity.[49] Progress has been made on developing computational methods to deal with amorphous materials.[50] Nonetheless, the crystalline set used in this study has helped demonstrate the key characteristics that can be tuned to optimize hydrogen storage.

In this work, we adopt a combination of thermodynamic models coupled with a neural network machine learning algorithm and a concise literature review to address the questions: what are the limits of hydrogen storage using porous materials and are there additional promising candidate materials to enhance the viability of a global hydrogen fuel economy?

While this manuscript was under review, two papers by Gomez-Gualdron et al. and Bobbitt et al. were published on the same topic showing the feasibility of molecular simulation for evaluating MOFs as cryo-adsorbents for hydrogen storage.[51,52] Our work differs from these studies by extending the approach to screen a much larger library of 850 000 materials and by using a combination of molecular simulation and machine learning. We also provide additional insights from calculations at room temperature and consider the energy cost of storage scenarios from an engineering perspective to compare methods on an even playing field.

2. METRIC FOR HYDROGEN STORAGE

Essential considerations for hydrogen to compete with conventional fossil-based fuels in the transportation sector are the volumetric and gravimetric storage density, refuelling infrastructure costs, recurring storage costs (e.g., to compress the hydrogen), fuel tanks costs, durability, and the time to store/release.[10] The hydrogen storage challenge for vehicular transport, set by the U.S. Department of Energy (U.S. DOE), focused a wide range of research disciplines toward the goal of densifying hydrogen for use as a transportation fuel.[53] The volumetric energy density, which primarily determines driving range[54] and cost of storage, has proven the more difficult of the requirements. The U.S. DOE quantified these requirements and set the progressive benchmarks that led to ultimate targets of 2.4 kW·h/L for volumetric energy density at a net cost of $8 per kW·h. Industry has less stringent guidelines, considering temperatures below −40 °C to produce liquid hydrogen and also above the pressure range considered safe, into the 700 bar region.[1,55] With industry setting new benchmarks, the most important requirements are net energy density and cost of storage. Here the

DOI: 10.1021/acs.chemmater.6b04933
Chem. Mater. 2017, 29, 2844−2854

net deliverable energy is defined as the electrical energy from desorbed H_2 minus the energy required to cool and compress H_2; see Supporting Information (SI) for complete details.

Liquefaction, compression, and cryo-compression are three storage methods of pure hydrogen that do not require other materials such as chemicals, chemi-sorbents, or physical adsorbents. Liquefaction of hydrogen requires cooling to 20 K at a cost of about 0.24 kW·h/L resulting in a theoretical net energy of 2.1 kW·h/L, while the actual net energy is around 1.7 kW·h/L depending on the method of liquefaction.[56,57] Pressurizing hydrogen at room temperature to 700 bar costs about 0.12 kW·h/L with a total net energy of 1.2 kW·h/L, assuming isothermal compression. Pressurization of hydrogen to 100 bar and cooling to cryogenic temperatures of 77 K, also known as cryo-compression, only costs about 0.03 kW·h/L with a total net energy of 1.02 kW·h/L. Details of calculations can be found in Table SI-1 using data from the National Institute of Standards and Technology (NIST).[58] In summary, liquefied hydrogen has the highest net volumetric energy followed by 700 bar compression at room temperature and finally moderate pressurization at cryogenic temperatures. Note that the opposite trend is found when considering the molar (or gravimetric) efficiency of storage, and these calculations do not consider the volume or mass of equipment such as the tank, compressors, insulation, valves, etc.

In reality, the most appropriate type of storage method is application-dependent. For example, storage for aviation applications will consider both gravimetric and volumetric energy densities as important but the cost not as critical, whereas a remote community will consider cost much more important than gravimetric or volumetric restrictions. Location and method of hydrogen production and the distribution network available for each application must also be considered. For example, hydrogen pipelines deliver compressed hydrogen over long distances without much loss, and liquefied hydrogen tankers can deliver where pipelines are not available but suffer loss from boil-off issues. This study aims to optimize volumetric storage at 100 bar and cryogenic temperatures, which is an important intermediate solution and is currently the most challenging regime.

3. NANOPOROUS MATERIALS GENOME (NMG)

The NMG consists of over 3 million structures including hypothetical MOFs,[16] computationally-ready experimental MOFs (CoRE-MOFs) taken from the Cambridge Structural Database (CSD),[21] hypothetical zeolites chosen from a set of energetically feasible structures from the Predicted Crystallography Open Database (PCOD),[17] ideal silica zeolites from the International Zeolite Association (IZA),[59] hypothetical covalent organic frameworks (COFs),[18] hypothetical zeolitic imidazolate frameworks (ZIFs) that are identical to hypothetical zeolites but with the Si−O bond replaced with Zn−imidazolate,[19] and hypothetical porous polymer networks (PPNs);[20] see Figure 1a. For a more detailed review of these materials, see ref 34.

CoRE-MOFs and IZA zeolites are the only experimentally derived materials considered in this study. Chung et al. developed the CoRE-MOF database by downloading all MOF structures from the CSD and automatically preparing the structures for molecular simulations, which involved removing solvent molecules and the resetting of partially occupied and disordered atoms.[21] The IZA zeolites contain about 200 experimentally observed structures, of which 30 have been synthesized in pure-silica form.

The synthetic feasibility of the hypothetical structures is difficult to determine. Most of the structures were constructed using simple, available, and known building blocks that are capable of forming MOFs. There are some experimentally confirmed MOFs in the hypothetical

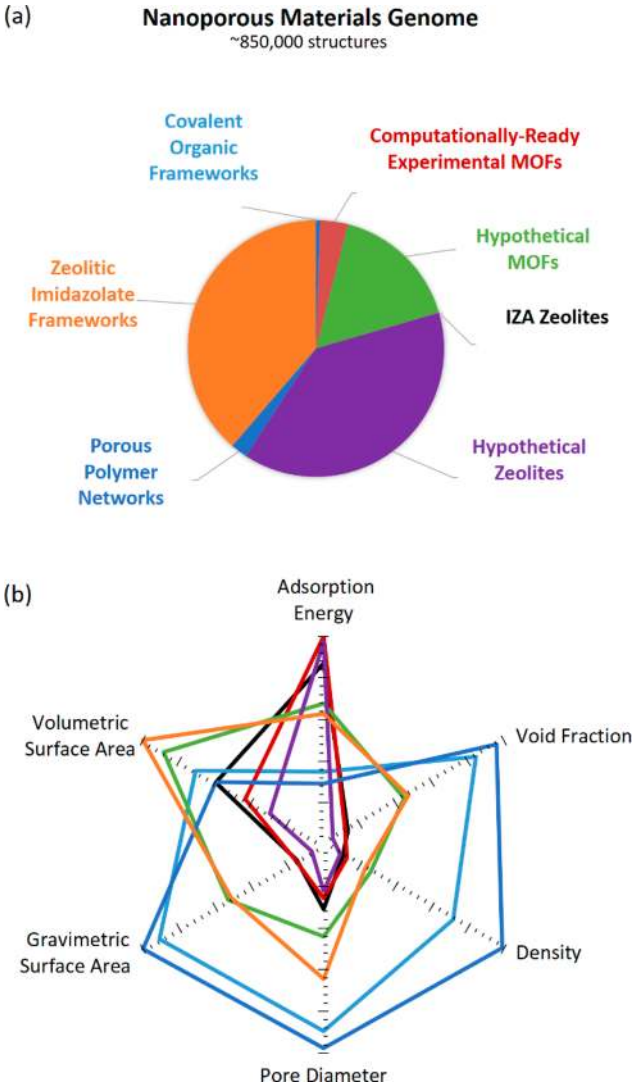

Figure 1. (a) Pie chart depicting classes of materials in the NMG, consisting of over 850 000 structures. (b) Structural parameter space represented as the average property normalized by the maximum average. For example, CoRE-MOFs have the highest average adsorption energy. Note that some data sets have some very wide distributions; see Table SI-3 for the statistics and Figure SI-7 for the complete graphical matrix of the structural parameters.

database, but no thorough analysis has been performed between the sets of structures. It is likely that there will be a problem synthesizing large pore MOFs where the rigidity of the framework is tested against thermodynamic forces and also for interpenetrated MOFs where sterically restricted growth is difficult to control.[60] However, it is possible to use the method developed by Raccuglia et al. to predict the success of reactions between inorganic and organic building blocks using machine learning trained on data from failed experiments.[61]

The size of chemical and parameter space explored by this data set of materials is large. For example, some of the PPNs have achieved surface areas of 10 000 m^2/g and pore diameters of 88 Å, well above the experimental average of 900 m^2/g and 5.4 Å according to the CoRE-MOF set. Table SI-3 lists the minimum, mean, median, and maximum values of each set of materials. Some metal centers can form much stronger interactions with H2 such as the europium-based MOF (refcode: CUFMOG) with one of the highest adsorption energies of 11 kJ/mol.

Here we screen over 850 000 materials in the NMG for hydrogen storage. The average properties for each category are depicted in Figure 1b. There are a few interesting observations to be made regarding

DOI: 10.1021/acs.chemmater.6b04933
Chem. Mater. 2017, 29, 2844−2854

the coverage of chemical space by different classes of materials. First, the experimental CoRE-MOFs have average characteristics similar to those of the zeolites, with small pore diameters, low density, low void fraction, and low surface areas compared to the hypothetical MOFs. This agrees with the general understanding that MOFs with large pores are difficult to synthesize because of the increased lattice energy with specific volume.[60] Nonetheless, a key difference between experimental MOFs and zeolites is that, in MOFs, high adsorption energies can be coupled with larger pores and higher void fractions because of the unique configurations of inorganic and organic components (see Figure SI-11). For example, bimetal indium and manganese MOF (CSD refcode: WAVRAO) has a potential adsorption energy of 4 kJ/mol coupled with a large pore diameter of 15 Å and void fraction of 0.3.[62] The data set of COFs and PPNs exhibits similar properties, understandable considering their purely organic nature and long molecular building blocks. Finally, the properties of the hypothetical ZIFs are similar to those of the hypothetical MOFs, again understandable considering that ZIFs are a subset of MOFs.

It is important to note that this is an early snapshot of the growing hypothetical and experimental porous materials genome database. Hypothetical MOFs,[16] for example, have only utilized 150 building blocks combined with a limited number of topologies, while the CSD shows there are a vast number of alternative organic and inorganic components with a greater variety of topologies.

4. SCREENING THE MATERIALS DATABASE

In silico screening is an approach that uses high-throughput, step-by-step predictive calculations of the properties of large numbers of materials to find promising candidates for a specific application.[63] Predictive calculations range from empirical models, such as those implemented by Goldsmith et al. based on surface area and pore volume,[64] to more fundamental approaches such as the Langmuir adsorption model and Monte Carlo simulations on the grand canonical ensemble (GCMC). Each approach has its own range of applicability depending on the temperature, pressure, and regime of pore size and interaction strength.[65] Simulations of adsorption using classic molecular models have proven accurate on a wide range of materials.[22,23,25,34,37] For example, predicting natural gas storage using a combination of simulation and analytical tools was validated using individual structures and found reliable for screening over 650 000 candidates.[34]

In this study, we predicted room temperature storage using the Langmuir adsorption model with input from simulations. Hydrogen uptake (N) is related to the Langmuir equilibrium constant (K), pressure (P), and saturation capacity (M) as follows,

$$N = \frac{KP}{1 + KP}M$$

The Langmuir constant is equal to the simulated Henry coefficient (k_H) divided by the saturation capacity. The Henry coefficient was calculated from Widom insertions described by Frenkel and Smit.[66] Saturation capacity was estimated as the product of pore volume (V_P) and hydrogen density (ρ). The density of liquid hydrogen at 70.8 g/L is a reasonable value for ρ;[67] however, using an empirical relationship between pore volume and hydrogen density improved R^2 for predicting simulated uptake using the Langmuir equation from 0.88 to 0.98 (see Figure SI-1).[19] The crystal density is used throughout this study, ignoring any packing effects within the tank, an ideal scenario with the intention to determine the limits of hydrogen storage. For conversion from ideal to actual uptake, one can assume a 25% loss in volumetric uptake.[54]

At cryogenic temperatures, the analytical Langmuir model failed to adequately predict adsorption capacity because of the poor correlation between hydrogen density and pore volume at high pressures. Therefore, we used GPU-based GCMC simulations to predict hydrogen uptake, using the code developed by Kim and Smit that enabled significant speedup (over 40 times) compared to the conventional non-GPU code.[68]

Force fields are required to describe the interactions between hydrogen and the adsorbent. Hydrogen was treated as a single Lennard-Jones sphere with the widely used Buch potential,[69] which shows excellent agreement with experimental hydrogen isotherms.[70] In this study the Universal Force Field (UFF)[71] was adopted. It is the most common force field for framework atoms in the literature, with reasonably good accuracy for MOFs according to a review by Basdogan and Keskin.[72] For zeolites this force field has also proven adequate under cryogenic conditions, with a slight improvement using modified UFF parameters; see Deeg et al.[73] When exploring a materials genome with over 850 000 structures, this can still be too computationally demanding. The genome is also continually growing, and therefore a smarter screening strategy than the conventional brute-force approach is required. Neural networks that progressively learn from data were incorporated into the workflow to reduce the computational time and to more rapidly converge on the top candidates.

Neural network models for gas adsorption were trained on data sets generated by GCMC to predict hydrogen adsorption capacity on the basis of structural descriptors in Figure 1b. The models were then used to target promising candidates in an evolutionary manner.[74] This process of simulation followed by neural network training and targeting continued until the predicted working capacity converged upon a maximum where no new candidates were identified. Bayesian regularized feed-forward neural networks were used to build the initial structure−property models to prevent overfitting and to remove any subjective bias.[43] They have been shown to generate robust, predictive models of a wide variety of materials properties. The networks employed input, hidden and output layers. The number of nodes in the input layer was the same as the number of descriptors, the number of hidden layer nodes was generally 2 or 3, and one output node was used.

Neural networks require a target property and quantitative descriptors. The target property in this case was the volumetric working capacity which was later converted to net energy by assuming that hydrogen produces 0.066 kW·h/mol of electrical energy (calculated from the Gibbs free energy function) at a cost of 0.03 kW·h/L; see Table SI-1. The chosen descriptors were those that could be rapidly calculated, such as adsorption energy (ensemble average at 77 K and infinite dilution), density, void fraction (geometrically calculated using Zeo++[75,76]), surface area (gravimetric and volumetric), and pore size (maximum). For more complex systems, such as biological interactions, more descriptors are required, but for gas adsorption a handful of descriptors has proven to be adequate.[22,24,40]

5. RESULTS AND DISCUSSION

For room temperature storage, the maximum net deliverable energy using adsorbents at pressures between 100 and 1 bar is about 0.4 kW·h/L, as shown in Figure 2 for the complete NMG (~850 000). Materials with a positive adsorption energy were omitted from the graph. This is well below the net energy delivered by high compression (700 bar) systems at 1.2 kW·h/L. Deliverable energy is maximized at void fractions of 0.1 and pore sizes of 6 Å; see Figure SI-5 for complete structure−property dependence. The optimal storage pressure can be calculated from the Langmuir equilibrium constant and the delivery pressure.

DOI: 10.1021/acs.chemmater.6b04933
Chem. Mater. 2017, 29, 2844−2854

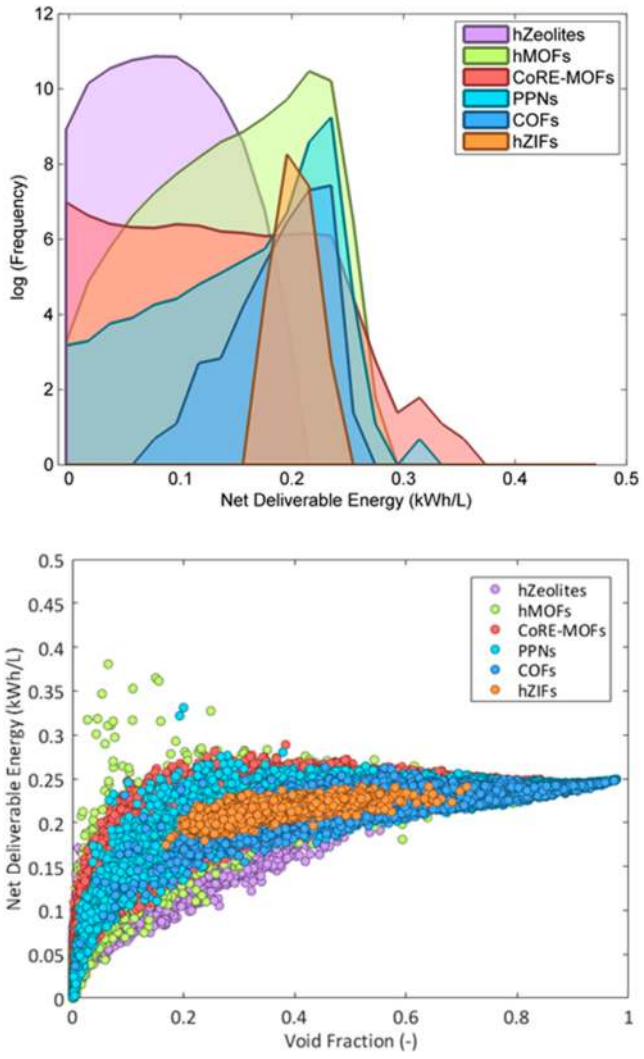

Figure 2. Room temperature simulations on the complete NMG (~850 000 materials). Net deliverable energy predicted at room temperature and cycling between 100 and 1 bar using the Langmuir model with simulated Henry coefficient and empirical relation for saturation capacity. (Top) Histogram of the net deliverable energy. (Bottom) Net deliverable energy versus void fraction.

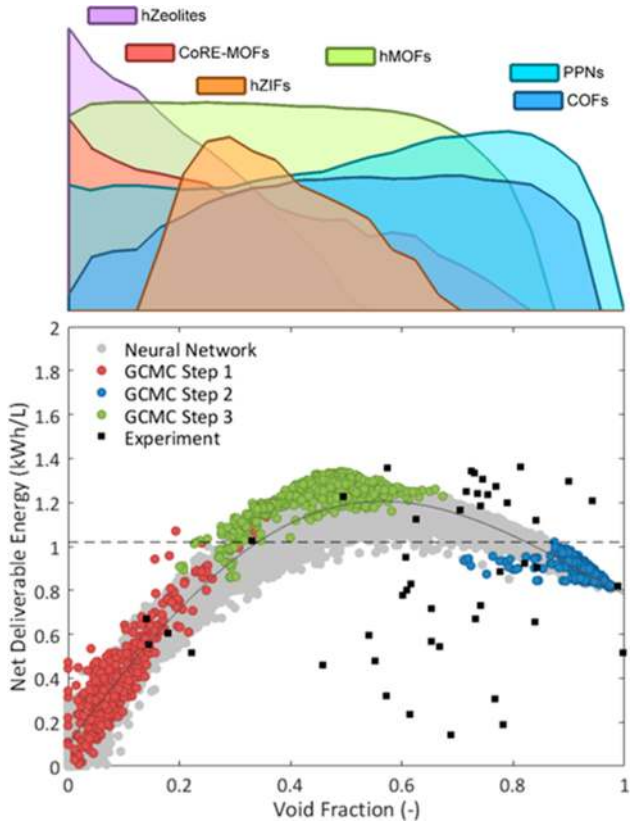

Figure 3. Net deliverable energy as a function of void fraction for the predictive and experimental data at 77 K cycling between 100 and 1 bar. Predictions include the GCMC-simulated sample sets and the final neural network model for the complete genome (~850 000 materials). Experimental data from the literature is shown as black squares with top candidates including NOTT-400, MOF-210, ZIF-8, and PCN-68. Dashed line represents the predicted bare tank performance based on NIST data. Solid dark gray line represents the fitted Langmuir model. Histograms of void fraction for each class of materials are shown above.

In this manner, the pressure required to maximize the net deliverable energy was calculated, accounting for the cost of pressurization. Optimization of storage pressure for the available adsorbents raises the net deliverable energy close to the DOE target; however, the pressures required are greater than 1000 bar (see Figure 2 and Figure SI-4). Therefore, it is likely more economical to operate without an adsorbent at room temperature.

At cryogenic temperatures, the Langmuir model coupled with a temperature-dependent K suggested that storage pressures as low as 10 bar can be optimal for some candidates; see Figure SI-4. Unfortunately, the Langmuir model was not accurate enough to predict the majority of isotherms at cryogenic temperatures. On the basis of this range, isotherms between 100 and 1 bar were simulated using GCMC, a more accurate method under these conditions. The simulations were run in stages, where results from each stage were fed into a neural network to generate models that identified the next set of materials to simulate.

The first stage of GCMC simulations was run on the complete set of known IZA zeolites and a diverse set of hypothetical zeolites selected on the basis of molecular similarity,[77] shown as red circles in Figure 3. A neural network model was then constructed, and a new set of materials with improved properties were identified; see Figure SI-6 for the complete set of predictions. The limited parameter space (domain of applicability) of zeolites meant that the neural network model suggested structures with the largest amount of void fraction, consisting of PPNs and COFs.

The top 1000 structures suggested by the neural model in the first stage were then simulated using GCMC, and the results are shown as blue circles in Figure 3. As expected, the difference between the stage 1 neural network predictions and the GCMC simulations were large because of the limited information used to train each neural network model. However, the new GCMC results were used to further retrain the neural model, and more complex relationships between the structural descriptors of the materials and performance were subsequently observed. For example, an optimal range was identified for each parameter, including a pore diameter of around 6 Å and surface area of 4000 $m^2 g^{-1}$. The range of materials found within these optimal ranges included a combination of hypothetical MOFs and CoRE-MOFs.

A third stage of GCMC simulations was run for the next top 1000 structures suggested by the neural model which was once again retrained on the new simulated data, shown as green

DOI: 10.1021/acs.chemmater.6b04933
Chem. Mater. 2017, 29, 2844−2854

circles in Figure 3. The new results identified an optimal range of void fraction around 0.5, highlighting a trade-off between free space for adsorbed H_2 molecules and a framework to construct binding sites with a high affinity for hydrogen. A final neural network model was developed with this additional simulation data that revealed a convergence in the list of top candidates; i.e., no new candidates were suggested. This can be seen in Figure 3 where the final neural model predictions are shown as pale gray circles.

To ensure that the neural network had a sufficiently large domain of applicability in the available parameter space, a diverse test set of candidates (based on molecular similarity)[77] was tested. No new high performing candidates were discovered, confirming that the neural network has captured enough of the parameter space to arrive at a good approximation of the global maximum. Furthermore, the neural network model predicted the performance of the diverse test set with good accuracy ($R^2 = 0.88$ and root mean squared error of 3.64), showing that it could accurately predict the properties of materials not used in the training set (see Figure SI-8 and Table SI-2).

The top candidates were predicted to deliver a net energy of around 1.3 kW·h/L, well above the bare tank option at 1.02 kW·h/L for the same operating conditions. Catenated hypothetical MOFs were the most common among the high performing candidates, along with CoRE-MOFs that will be discussed below. Compared to current industrial practice, this maximum net deliverable energy by adsorbents is higher than the 700 bar compression technology (1.2 kW·h/L) but lower than the liquefaction option (2.1 kW·h/L). The advantage of cryo-adsorption is clearly in applications where high pressures (700 bar) and low temperatures (20 K) are not appropriate due to safety, source of hydrogen, available floor space, engineering factors, cost, or other restrictions. For example, adsorbents can reduce the high pressures in confined spaces, which are considered unsafe or at least undesirable although carbon fiber composites are raising the reliability of storage tanks. Another example to consider is for locations with access to liquid nitrogen but not the equipment required to produce liquid hydrogen. In this example, adsorbents will offer the additional storage performance. Hydrolyzers produce hydrogen at high temperatures, and therefore another opportunity for adsorbents could be to adsorb this hydrogen along heat exchangers.

To better understand this predicted peak in net energy at an optimal void fraction of 0.5, the Langmuir model was fitted to the final neural network predictions (solid dark gray line in Figure 3). By simply assuming that the saturation capacity and adsorption energy are linear functions of void fraction, the data were fitted with high accuracy ($R^2 = 0.985$). These generalized semiempirical relationships were observed previously, and the trends are confirmed in this work.[19,78,79] Saturation capacity is an increasing function of void fraction while adsorption energy (represented as positive values, where a large positive value is a strong attractive adsorption energy) is a decreasing function of void fraction. This model intuitively captures the natural trade-off between saturation capacity and adsorption energy, which are proportional to and inversely related to void fraction, respectively.

Although void fraction plays a critical role in maximizing deliverable capacity, other parameters also contribute to an optimum range as shown in Figure SI-6. An optimal adsorption energy of around −2 kJ/mol can be found (see Figure SI-10) along with optimum framework density at 2 cm^3/g, pore diameter at 10 Å, gravimetric surface area at 5000 m^2/g, and volumetric surface area at 3000 cm^2/m^3. It is important to note that there are significant correlations between all parameters, as shown in Figure SI-7. Therefore, it may be possible to simplify future screening using a single screening parameter such as void fraction. However, other parameters could also be used, such as fractional volume for adsorption defined by Thornton et al.[80] or binding fraction by Bobbitt et al.[52]

It is important to note that the optimum value for each parameter depends on the adsorption/desorption conditions and the method by which the parameters are calculated. In this study, void fraction is calculated geometrically using Voronoi maps through the Zeo++ package[75,76] while other studies have used Widom insertions of a helium probe which can give very different values.[51,52] Bobbitt et al.[52] and Gomez-Gualdron et al.[51] also based their studies on different adsorption/desorption conditions along with molar volumes from Standard Temperature and Pressure (STP) instead of Standard Ambient Temperature and Pressure (SATP) which is likely to explain any discrepancy between the reported maximum deliverable capacities.

The predicted limit is based on the materials currently available within the genome. With a growing number of structures, it is important to understand the theoretical limits of hydrogen storage. In this case a purely fictitious material is considered with infinite pore volume, i.e., 100% void space, and with a tunable adsorption energy to achieve the optimal Langmuir equilibrium constant described previously. A maximum saturation capacity of 130 g/L is assumed from a simple packing of hydrogen as "hard-spheres". In this ideal scenario, the theoretical maximum energy deliverable between 100 and 1 bar is 3.5 kW·h/L, about 2.5 times above the observed limit. It is difficult to predict how much closer adsorbents will get to this theoretical limit given the natural trade-off between adsorption energy and void fraction.

Experimental data were collected from a range of reviews including Sculley et al.,[9] Suh et al.,[8] Yang et al.,[10] Hu et al.,[11] Lai et al.,[7] and Murray et al.[12] A selection is plotted in Figure 3 as black squares. Although there is significant scatter across void fraction and deliverable capacity, a maximum is also observed close to that of the predictions at around 1.3 kW·h/L. Top candidates include MOF-210,[81] NOTT-400,[82] PCN-68,[83] and ZIF-8.[84] The reason for discrepancies between simulation and experiment is often difficult to identify because of the multiple and interdependent variables involved in the synthesis and measurements, as well as the assumptions behind the simulations. Adsorption in ZIF-8 has proven difficult to predict due to observed "gate-opening" effects whereby the imidazole groups rotate at high pressures to adsorb more gas.[85] Adsorption in MOF-210 has also proven difficult to predict because of its large unit cell containing 5562 atoms.[81] Nonetheless, Figure 4 shows the comparison of top candidates with experimental data along with the bare tank scenario.

Reasonably good agreement is found between GCMC and experimental data for MOF-210 and ZIF-8. Although the general isotherm trend for ZIF-8 is captured, the working capacity is underpredicted because of the slight over and under predictions at 1 and 100 bar, respectively, possibly due to the absence of molecular flexibility in the simulation. PCN-68 depicts a similar isotherm to that of MOF-210, where a large uptake is observed at higher pressures.[83] A key feature for the top performing candidates is a combination of minimal uptake at delivery pressures (1 bar) and maximum uptake at storage pressures (100 bar). This feature is demonstrated in Figure 5 for hypothetical MOF-5059389 with the highest working capacity of

DOI: 10.1021/acs.chemmater.6b04933
Chem. Mater. 2017, 29, 2844−2854

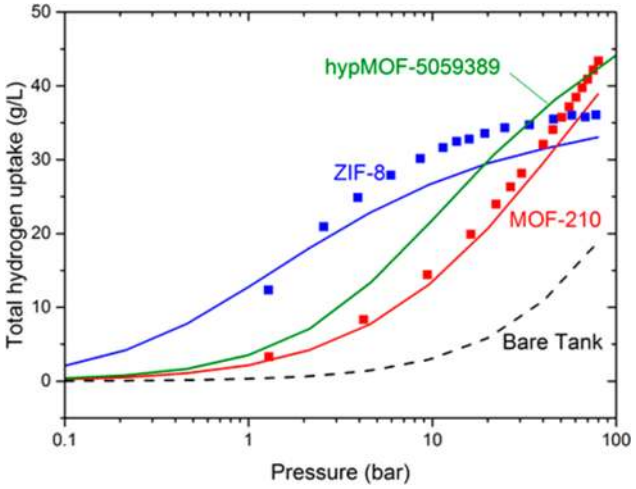

Figure 4. Total hydrogen uptake for top candidates with the highest working capacity including MOF-210,[81] ZIF-8,[84] and hypothetical MOF-5059389, along with the bare tank scenario. GCMC simulations (lines) and experimental data (squares) at 77 K.

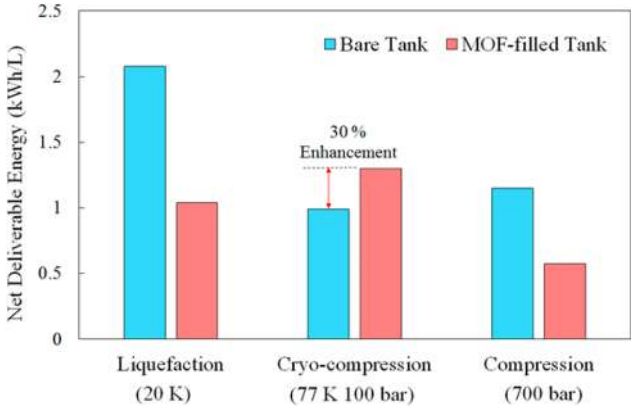

Figure 5. Net deliverable energy with and without MOF for the available storage conditions associated with liquefaction, cryo-compression, and compression. Top hypothetical candidate hypMOF-5059389 is chosen for comparison. The 30% enhancement is observed for the MOF-filled tank at cryo-compression conditions which corresponds to about 30% enhancement in volumetric capacity to 40 g/L.

40 H_2 g/L identified in the NMG database. This corresponds to a 30% enhancement above the bare tank scenario. Liquefaction remains the most efficient method of storage based on theoretical calculations. However, in reality liquefaction costs 24% more than the theoretical value, which means MOF-based cryo-adsorption is a promising alternative.

The top candidates including two hypothetical MOFs, two CoRE-MOFs with no known experimental hydrogen uptake, and two CoRE-MOFs where experimental hydrogen uptake is available are illustrated in Figure 6. The top hypothetical MOF candidates contain long and thin ligands such as alkynes that maximize surface area and porosity. hypMOF-5003600 is an interpenetrated zinc-based cubic framework while hypMOF-5059389 is functionalized with hydroxyl groups, and both strategies are typically adopted to maximize adsorption energy. CoRE-MOF candidates include cadmium-based MOF (CSD refcode: KECRAL10) linked with cyanide that forms an open framework with hexagonal and square-shaped channels.[86] An additional CoRE-MOF (CSD refcode: GUNFAW01) was found with mixed-metal vertices (chromium and manganese)

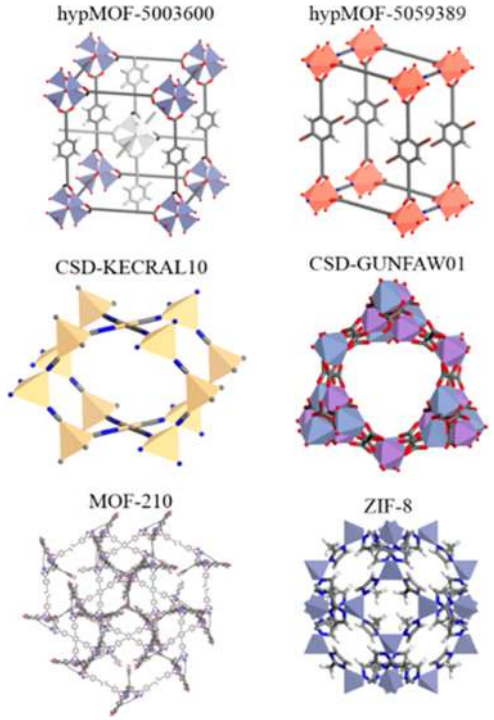

Figure 6. Top candidates for hydrogen storage at 77 K. Structures include two hypothetical MOFs that have never been synthesized, two MOFs from the CSD that were synthesized but never tested for hydrogen storage,[86,87] and two MOFs that have been synthesized and measured for hydrogen storage.[81,84] The color code for atoms: Zn (lavender), Cd (yellow), C (gray), O(red), N (blue), H (white), Cr (violet), Mn (dark-blue), and Cu (orange).

linked with bipyridine and phenylpyridine that was originally designed to exhibit specific magnetic properties.[87] A contour plot of the predicted volumetric uptake for candidate GUNFAW01 across all temperatures and pressures can be found in Figure SI-9. The top candidates share common characteristics such as a void fraction close to 0.5 and a major pore diameter of around 10 Å, along with high surface areas above 3000 cm^2/cm^3 and 5000 m^2/g. The exception is MOF-210 with a wide distribution of pores from 10 up to 28 Å.

An important conclusion of this study is that most of the top candidates for hydrogen storage have already been synthesized and tested. This result gives credit to the research community, which has strategically identified structures that maximize hydrogen storage. Although many candidates are predicted to perform at a similar level, there are no candidates predicted to outperform the current candidates available.

These calculations are based on physical adsorption by rigid structures, while there is much development in switchable structures under an external stimuli such as light, pressure, temperature, humidity, sound, magnetic fields, and others.[60,88,89] These dynamic structures show great promise for the low energy release of stored hydrogen, especially where uptake is enhanced at higher pressures (storage conditions) and minimized at lower pressures (delivery conditions); hence, the working capacity is maximized.

Chemisorbents are also not considered in this study because of the inability to cycle with pressure without the loss of hydrogen, as indicated by DOE studies on metal hydrides.[53] However, it is worth considering that there is no clear distinction between physisorption and chemisorption. This has been demonstrated

DOI: 10.1021/acs.chemmater.6b04933
Chem. Mater. 2017, 29, 2844−2854

by McDonald et al. for CO_2 capture where a slight change in pressure can induce chemisorbed species to desorb within short time frames.[90] In addition, Colón et al.[25] calculated the adsorption energy with magnesium alkoxide to be around 30 kJ/mol which is intermediate between that found in physisorbents (~10 kJ/mol) and that found in chemisorbents (~60 kJ/mol).[7]

Mechanical, chemical, hydrolytic, and thermal stability that can significantly effect adsorption performance throughout the product lifecycle are also important properties to consider.[91−93] Reviews on the stability of physisorbents can be used as a guide in selecting stable structures from the genome. However, robust computational models of stability that can be applied to large-scale screening studies are desirable.[92,94]

Industry will be driven by the economic advantages of using sorbents. According to a recent techno-economic analysis of sorbents, the baseline cost of MOF production is between 35 and 72 USD/kg.[95] Carbon fiber-based hydrogen storage tanks cost around 600 USD/kgH_2 according to a DOE report.[96] Considering the baseline cost of MOF along with the predicted storage enhancement of 30%, the total tank cost would range from 560 to 704 USD/kgH_2. Therefore, as a rough estimate, the cost of MOF production must be kept below 45 USD/kg to be economical with current technologies.

6. CONCLUSION

The nanoporous materials genome, consisting of over 850 000 crystalline structures, was computationally screened using a combination of molecular simulation and machine learning techniques to explore the limits of physisorbed hydrogen storage. Analysis of the genome revealed that CoRE-MOFs have a wider range of characteristics than zeolites including higher adsorption energies coupled with greater void space, hypothetical MOFs offer the best combination of adsorption energy and volumetric surface area, and PPNs and COFs have the largest void fractions. Neural networks were found to accelerate the identification of improved materials by learning from GCMC-simulated hydrogen isotherms in a kind of adaptive evolution process.

With a focus on the net energy derived from working capacity between 100 and 1 bar, optimal candidates were discovered that consisted of a collection of hypothetical MOFs and CoRE-MOFs found in experimental databases. MOF-210, PCN-68, NOTT-400, and ZIF-8 were four of the best materials identified, and experimental validation for their high hydrogen storage performance was found in the literature. Other top candidates included MOFs that have been synthesized in the literature but not yet measured for hydrogen capacity, such as the cadmium-based framework and the mixed-metal chromium−manganese based framework. Finally, hypothetical MOF candidates with a combination of large void fraction and high adsorption energy were also predicted to perform at a high level. Optimal characteristics were determined, including a void fraction of 0.5, a pore diameter of 10 Å, and a surface area of 5000 m^2/g, which offer quantitative guidelines for the future design of nanoporous materials for hydrogen storage.

Finally, the maximum net deliverable energy was found to be around 1.3 kW·h/L, which is well above the 1.02 kW·h/L for the bare tank scenario at identical operating conditions, 1 to 100 bar at 77 K. In addition, this technology termed "cryo-adsorption" has significant engineering advantages over the current liquefaction (20 K) and mega-compression (700 bar) storage technologies.

■ ASSOCIATED CONTENT

Supporting Information

The Supporting Information is available free of charge on the ACS Publications website at DOI: 10.1021/acs.chemmater.6b04933.

Langmuir model with simulated Henry's coefficient and saturation capacity, cost of cooling and compression, maximization of net deliverable energy, extension of Langmuir model to cryogenic temperatures, and Feynman Hibbs correction for quantum effects (PDF)

■ AUTHOR INFORMATION

Corresponding Author

*(A.W.T.) E-mail: Aaron.Thornton@csiro.au.

ORCID

Aaron W. Thornton: 0000-0002-7959-1397
David A. Winkler: 0000-0002-7301-6076
Berend Smit: 0000-0003-4653-8562

Author Contributions

The manuscript was written through contributions of all authors. All authors have given approval to the final version of the manuscript.

Notes

The authors declare no competing financial interest.
Complete data set for download: http://research.csiro.au/virtualscreening.

■ ACKNOWLEDGMENTS

A.W.T. acknowledges the support from the CSIRO Computational & Simulations Sciences and the Julius Award. M. Haranczyk gratefully acknowledges research support from the U.S. Department of Energy, Office of Energy Efficiency and Renewable Energy, Fuel Cell Technologies Office, under Contract No. DE-AC02-05CH11231. B.S. and C.S. are supported by the Center for Gas Separations Relevant to Clean Energy Technologies, an Energy Frontier Research Center funded by the U.S. DOE, Office of Science, Office of Basic Energy Sciences, under Award No. DE-SC0001015. B.S. received funding from the European Research Council under the European Union's Seventh Framework Programme (FP/2007-2013)/ERC Grant Agreement No. 666983 (MaGic). K.D. acknowledges support from NSF Graduate Research Fellowships. J.K. and B.S. acknowledge support of the Korean-Swiss Science and Technology Programme (KSSTP) grant number 162130 of the Swiss National Science Foundation (SNSF). This research was also supported by the International Research & Development Program of National Research Foundation of Korea (NRF) funded by the Ministry of Science, ICT & Future Planning (Grant number: 2015K1A3A1A14003244).

■ ABBREVIATIONS

NMG, nanoporous materials genome; MOF, metal−organic framework; U.S. DOE, U.S. Department of Energy; NIST, National Institute of Standards and Technology; CoRE-MOF, computationally ready experimental metal−organic framework; CSD, Cambridge Structural Database; PCOD, Predicted Crystallography Open Database; COF, covalent organic framework; ZIF, zeolitic imidazolate framework; PPN, porous polymer network; GCMC, grand canonical Monte Carlo; UFF, universal force field

DOI: 10.1021/acs.chemmater.6b04933
Chem. Mater. 2017, 29, 2844−2854

REFERENCES

(1) Eberle, U.; Muller, B.; von Helmolt, R. Fuel Cell Electric Vehicles and Hydrogen Infrastructure: Status 2012. *Energy Environ. Sci.* **2012**, *5* (10), 8780−8798.

(2) Offer, G. J.; Howey, D.; Contestabile, M.; Clague, R.; Brandon, N. P. Comparative Analysis of Battery Electric, Hydrogen Fuel Cell and Hybrid Vehicles in a Future Sustainable Road Transport System. *Energy Policy* **2010**, *38* (1), 24−29.

(3) Crabtree, G. W.; Dresselhaus, M. S.; Buchanan, M. V. The Hydrogen Economy. *Phys. Today* **2004**, *57* (12), 39−44.

(4) *Inventory of U.S. Greenhouse Gas Emissions and Sinks*; U.S. Environmental Protection Agency: 2015.

(5) Miller, E. L. Photoelectrochemical Water Splitting. *Energy Environ. Sci.* **2015**, *8* (10), 2809−2810.

(6) Durbin, D. J.; Malardier-Jugroot, C. Review of Hydrogen Storage Techniques For on board Vehicle Applications. *Int. J. Hydrogen Energy* **2013**, *38* (34), 14595−14617.

(7) Lai, Q.; Paskevicius, M.; Sheppard, D. A.; Buckley, C. E.; Thornton, A. W.; Hill, M. R.; Gu, Q.; Mao, J.; Huang, Z.; Liu, H. K.; Guo, Z.; Banerjee, A.; Chakraborty, S.; Ahuja, R.; Aguey-Zinsou, K.-F. Hydrogen Storage Materials for Mobile and Stationary Applications: Current State of the Art. *ChemSusChem* **2015**, *8* (17), 2789−2825.

(8) Suh, M. P.; Park, H. J.; Prasad, T. K.; Lim, D.-W. Hydrogen Storage in Metal−Organic Frameworks. *Chem. Rev.* **2012**, *112* (2), 782−835.

(9) Sculley, J.; Yuan, D.; Zhou, H.-C. The Current Status of Hydrogen Storage in Metal-Organic Frameworks-Updated. *Energy Environ. Sci.* **2011**, *4* (8), 2721−2735.

(10) Yang, J.; Sudik, A.; Wolverton, C.; Siegel, D. J. High Capacity Hydrogen Storage Materials: Attributes for Automotive Applications and Techniques for Materials Discovery. *Chem. Soc. Rev.* **2010**, *39* (2), 656−675.

(11) Hu, Y. H.; Zhang, L. Hydrogen Storage in Metal−Organic Frameworks. *Adv. Mater.* **2010**, *22* (20), E117−E130.

(12) Murray, L. J.; Dinca, M.; Long, J. R. Hydrogen Storage in Metal-Organic Frameworks. *Chem. Soc. Rev.* **2009**, *38* (5), 1294.

(13) Jain, A.; Ong, S. P.; Hautier, G.; Chen, W.; Richards, W. D.; Dacek, S.; Cholia, S.; Gunter, D.; Skinner, D.; Ceder, G.; Persson, K. A. Commentary: The Materials Project: A Materials Genome Approach to Accelerating Materials Innovation. *APL Mater.* **2013**, *1* (1), 011002.

(14) Kali, T.; Wadia, C.; 2011. https://obamawhitehouse.archives.gov/blog/2011/06/24/materials-genome-initiative-renaissance-american-manufacturing.

(15) Nanoporous Materials Genome Center. http://www.chem.umn.edu/nmgc/.

(16) Wilmer, C. E.; Leaf, M.; Lee, C. Y.; Farha, O. K.; Hauser, B. G.; Hupp, J. T.; Snurr, R. Q. Large-Scale Screening of Hypothetical Metal-Organic Frameworks. *Nat. Chem.* **2011**, *4* (2), 83−89.

(17) Deem, M. W.; Pophale, R.; Cheeseman, P. A.; Earl, D. J. Computational Discovery of New Zeolite-Like Materials. *J. Phys. Chem. C* **2009**, *113* (51), 21353−21360.

(18) Martin, R. L.; Simon, C. M.; Medasani, B.; Britt, D. K.; Smit, B.; Haranczyk, M. In Silico Design of Three-Dimensional Porous Covalent Organic Frameworks Via Known Synthesis Routes and Commercially Available Species. *J. Phys. Chem. C* **2014**, *118* (41), 23790−23802.

(19) Lin, L.-C.; Berger, A. H.; Martin, R. L.; Kim, J.; Swisher, J. A.; Jariwala, K.; Rycroft, C. H.; Bhown, A. S.; Deem, M. W.; Haranczyk, M.; Smit, B. In Silico Screening of Carbon-Capture Materials. *Nat. Mater.* **2012**, *11* (7), 633−641.

(20) Martin, R. L.; Simon, C. M.; Smit, B.; Haranczyk, M. In Silico Design of Porous Polymer Networks: High-Throughput Screening for Methane Storage Materials. *J. Am. Chem. Soc.* **2014**, *136* (13), 5006−5022.

(21) Chung, Y. G.; Camp, J.; Haranczyk, M.; Sikora, B. J.; Bury, W.; Krungleviciute, V.; Yildirim, T.; Farha, O. K.; Sholl, D. S.; Snurr, R. Q. Computation-Ready, Experimental Metal−Organic Frameworks: A Tool to Enable High-Throughput Screening of Nanoporous Crystals. *Chem. Mater.* **2014**, *26* (21), 6185−6192.

(22) Simon, C. M.; Mercado, R.; Schnell, S. K.; Smit, B.; Haranczyk, M. What Are the Best Materials to Separate a Xenon/Krypton Mixture? *Chem. Mater.* **2015**, *27* (12), 4459−4475.

(23) Bai, P.; Jeon, M. Y.; Ren, L.; Knight, C.; Deem, M. W.; Tsapatsis, M.; Siepmann, J. I. Discovery of Optimal Zeolites for Challenging Separations and Chemical Transformations Using Predictive Materials Modeling. *Nat. Commun.* **2015**, *6*, 5912.

(24) Thornton, A. W.; Winkler, D. A.; Liu, M. S.; Haranczyk, M.; Kennedy, D. F. Towards Computational Design of Zeolite Catalysts for Co2 Reduction. *RSC Adv.* **2015**, *5* (55), 44361−44370.

(25) Colón, Y. J.; Fairen-Jimenez, D.; Wilmer, C. E.; Snurr, R. Q. High-Throughput Screening of Porous Crystalline Materials for Hydrogen Storage Capacity near Room Temperature. *J. Phys. Chem. C* **2014**, *118* (10), 5383−5389.

(26) Lee, K.; Howe, J. D.; Lin, L.-C.; Smit, B.; Neaton, J. B. Small-Molecule Adsorption in Open-Site Metal−Organic Frameworks: A Systematic Density Functional Theory Study for Rational Design. *Chem. Mater.* **2015**, *27* (3), 668−678.

(27) Bao, Y.; Martin, R. L.; Haranczyk, M.; Deem, M. W. In Silico Prediction of Mofs with High Deliverable Capacity or Internal Surface Area. *Phys. Chem. Chem. Phys.* **2015**, *17* (18), 11962−11973.

(28) Matito-Martos, I.; Martin-Calvo, A.; Gutierrez-Sevillano, J. J.; Haranczyk, M.; Doblare, M.; Parra, J. B.; Ania, C. O.; Calero, S. Zeolite Screening for the Separation of Gas Mixtures Containing So2, Co2 and Co. *Phys. Chem. Chem. Phys.* **2014**, *16* (37), 19884−19893.

(29) Evans, J. D.; Huang, D. M.; Hill, M. R.; Sumby, C. J.; Sholl, D. S.; Thornton, A. W.; Doonan, C. J. Molecular Design of Amorphous Porous Organic Cages for Enhanced Gas Storage. *J. Phys. Chem. C* **2015**, *119* (14), 7746−7754.

(30) Wang, B.; Truhlar, D. G. Screened Electrostatic Interactions in Molecular Mechanics. *J. Chem. Theory Comput.* **2014**, *10* (10), 4480−4487.

(31) Lin, L.-C.; Lee, K.; Gagliardi, L.; Neaton, J. B.; Smit, B. Force-Field Development from Electronic Structure Calculations with Periodic Boundary Conditions: Applications to Gaseous Adsorption and Transport in Metal−Organic Frameworks. *J. Chem. Theory Comput.* **2014**, *10* (4), 1477−1488.

(32) Simon, C. M.; Kim, J.; Lin, L.-C.; Martin, R. L.; Haranczyk, M.; Smit, B. Optimizing Nanoporous Materials for Gas Storage. *Phys. Chem. Chem. Phys.* **2014**, *16* (12), 5499−5513.

(33) Haranczyk, M.; Lin, L.-C.; Lee, K.; Martin, R. L.; Neaton, J. B.; Smit, B. Methane Storage Capabilities of Diamond Analogues. *Phys. Chem. Chem. Phys.* **2013**, *15* (48), 20937−20942.

(34) Simon, C. M.; Kim, J.; Gomez-Gualdron, D. A.; Camp, J. S.; Chung, Y. G.; Martin, R. L.; Mercado, R.; Deem, M. W.; Gunter, D.; Haranczyk, M.; Sholl, D. S.; Snurr, R. Q.; Smit, B. The Materials Genome in Action: Identifying the Performance Limits for Methane Storage. *Energy Environ. Sci.* **2015**, *8*, 1190−1199.

(35) Zhang, Y.; Yang, S.; Jiao, Y.; Liu, H.; Yuan, H.; Lu, S.; Ran, T.; Yao, S.; Ke, Z.; Xu, J.; Xiong, X.; Chen, Y.; Lu, T. An Integrated Virtual Screening Approach for Vegfr-2 Inhibitors. *J. Chem. Inf. Model.* **2013**, *53* (12), 3163−3177.

(36) Canepa, P.; Arter, C. A.; Conwill, E. M.; Johnson, D. H.; Shoemaker, B. A.; Soliman, K. Z.; Thonhauser, T. High-Throughput Screening of Small-Molecule Adsorption in Mof. *J. Mater. Chem. A* **2013**, *1* (43), 13597−13604.

(37) Wilmer, C. E.; Farha, O. K.; Bae, Y.-S.; Hupp, J. T.; Snurr, R. Q. Structure-Property Relationships of Porous Materials for Carbon Dioxide Separation and Capture. *Energy Environ. Sci.* **2012**, *5* (12), 9849−9856.

(38) Thornton, A. W.; Dubbeldam, D.; Liu, M. S.; Ladewig, B. P.; Hill, A. J.; Hill, M. R. Feasibility of Zeolitic Imidazolate Framework Membranes for Clean Energy Applications. *Energy Environ. Sci.* **2012**, *5* (6), 7637−7646.

(39) Dubbeldam, D.; Krishna, R.; Calero, S.; Yazaydın, A. Ö. Computer-Assisted Screening of Ordered Crystalline Nanoporous Adsorbents for Separation of Alkane Isomers. *Angew. Chem., Int. Ed.* **2012**, *51* (47), 11867−11871.

DOI: 10.1021/acs.chemmater.6b04933
Chem. Mater. 2017, 29, 2844−2854

(40) Fernandez, M.; Woo, T. K.; Wilmer, C. E.; Snurr, R. Q. Large-Scale Quantitative Structure−Property Relationship (Qspr) Analysis of Methane Storage in Metal−Organic Frameworks. *J. Phys. Chem. C* **2013**, *117* (15), 7681−7689.
(41) Burbidge, R.; Trotter, M.; Buxton, B.; Holden, S. Drug Design by Machine Learning: Support Vector Machines for Pharmaceutical Data Analysis. *Comput. Chem.* **2001**, *26* (1), 5−14.
(42) Epa, V. C.; Yang, J.; Mei, Y.; Hook, A. L.; Langer, R.; Anderson, D. G.; Davies, M. C.; Alexander, M. R.; Winkler, D. A. Modelling Human Embryoid Body Cell Adhesion to a Combinatorial Library of Polymer Surfaces. *J. Mater. Chem.* **2012**, *22* (39), 20902−20906.
(43) Le, T.; Epa, V. C.; Burden, F. R.; Winkler, D. A. Quantitative Structure−Property Relationship Modeling of Diverse Materials Properties. *Chem. Rev.* **2012**, *112* (5), 2889−2919.
(44) Salahinejad, M.; Le, T. C.; Winkler, D. A. Aqueous Solubility Prediction: Do Crystal Lattice Interactions Help? *Mol. Pharmaceutics* **2013**, *10* (7), 2757−2766.
(45) King, R. D.; Muggleton, S. H.; Srinivasan, A.; Sternberg, M. J. Structure-Activity Relationships Derived by Machine Learning: The Use of Atoms and Their Bond Connectivities to Predict Mutagenicity by Inductive Logic Programming. *Proc. Natl. Acad. Sci. U. S. A.* **1996**, *93* (1), 438−442.
(46) Fernandez, M.; Boyd, P. G.; Daff, T. D.; Aghaji, M. Z.; Woo, T. K. Rapid and Accurate Machine Learning Recognition of High Performing Metal Organic Frameworks for Co2 Capture. *J. Phys. Chem. Lett.* **2014**, *5* (17), 3056−3060.
(47) Epa, V. C.; Hook, A. L.; Chang, C.; Yang, J.; Langer, R.; Anderson, D. G.; Williams, P.; Davies, M. C.; Alexander, M. R.; Winkler, D. A. Modelling and Prediction of Bacterial Attachment to Polymers. *Adv. Funct. Mater.* **2014**, *24* (14), 2085−2093.
(48) Rossetti, I.; Ramis, G.; Gallo, A.; Di Michele, A. Hydrogen Storage over Metal-Doped Activated Carbon. *Int. J. Hydrogen Energy* **2015**, *40* (24), 7609−7616.
(49) Konstas, K.; Taylor, J. W.; Thornton, A. W.; Doherty, C. M.; Lim, W. X.; Bastow, T. J.; Kennedy, D. F.; Wood, C. D.; Cox, B. J.; Hill, J. M.; Hill, A. J.; Hill, M. R. Lithiated Porous Aromatic Frameworks with Exceptional Gas Storage Capacity. *Angew. Chem., Int. Ed.* **2012**, *51*, 6639−6642.
(50) Thornton, A. W.; Jelfs, K. E.; Konstas, K.; Doherty, C. M.; Hill, A. J.; Cheetham, A. K.; Bennett, T. D. Porosity in Metal-Organic Framework Glasses. *Chem. Commun.* **2016**, *52* (19), 3750−3753.
(51) Gomez-Gualdron, D. A.; Colon, Y. J.; Zhang, X.; Wang, T. C.; Chen, Y.-S.; Hupp, J. T.; Yildirim, T.; Farha, O. K.; Zhang, J.; Snurr, R. Q. Evaluating Topologically Diverse Metal-Organic Frameworks for Cryo-Adsorbed Hydrogen Storage. *Energy Environ. Sci.* **2016**, *9* (10), 3279−3289.
(52) Bobbitt, N. S.; Chen, J.; Snurr, R. Q. High-Throughput Screening of Metal−Organic Frameworks for Hydrogen Storage at Cryogenic Temperature. *J. Phys. Chem. C* **2016**, *120* (48), 27328−27341.
(53) Multi-Year Research, Development and Demonstration Plan - Planned Program Activities for 2003−2010: Technical Plan; U.S. Department of Energy; http://www.eere.energy.gov/hydrogenandfuelcells/mypp/pdfs/storage.pdf.
(54) Mason, J. A.; Veenstra, M.; Long, J. R. Evaluating Metal-Organic Frameworks for Natural Gas Storage. *Chemical Science* **2014**, *5* (1), 32−51.
(55) Hua, T.; Ahluwalia, R.; Eudy, L.; Singer, G.; Jermer, B.; Asselin-Miller, N.; Wessel, S.; Patterson, T.; Marcinkoski, J. Status of Hydrogen Fuel Cell Electric Buses Worldwide. *J. Power Sources* **2014**, *269*, 975−993.
(56) Gardiner, M. *Energy Requirements for Hydrogen Gas Compression and Liquefaction as Related to Vehicle Storage Needs*; 9013; U.S. Department of Energy: 2009.
(57) Züttel, A.; Borgschulte, A.; Schlapbach, L. *Hydrogen as a Future Energy Carrier*; Wiley: 2008.
(58) Linstrom, P. J.; Mallard, W. G. Nist Chemistry Webbook, Standard Reference Database Number 69. http://webbook.nist.gov/chemistry/.
(59) Baerlocher, C.; McCusker, L. B. Database of Zeolite Structures. www.iza-structure.org/databases/.
(60) Coudert, F.-X. Responsive Metal−Organic Frameworks and Framework Materials: Under Pressure, Taking the Heat, in the Spotlight, with Friends. *Chem. Mater.* **2015**, *27* (6), 1905−1916.
(61) Raccuglia, P.; Elbert, K. C.; Adler, P. D. F.; Falk, C.; Wenny, M. B.; Mollo, A.; Zeller, M.; Friedler, S. A.; Schrier, J.; Norquist, A. J. Machine-Learning-Assisted Materials Discovery Using Failed Experiments. *Nature* **2016**, *533* (7601), 73−76.
(62) Zheng, S.-T.; Wu, T.; Chou, C.; Fuhr, A.; Feng, P.; Bu, X. Development of Composite Inorganic Building Blocks for Mofs. *J. Am. Chem. Soc.* **2012**, *134* (10), 4517−4520.
(63) Colon, Y. J.; Snurr, R. Q. High-Throughput Computational Screening of Metal-Organic Frameworks. *Chem. Soc. Rev.* **2014**, *43* (16), 5735−5749.
(64) Goldsmith, J.; Wong-Foy, A. G.; Cafarella, M. J.; Siegel, D. J. Theoretical Limits of Hydrogen Storage in Metal−Organic Frameworks: Opportunities and Trade-Offs. *Chem. Mater.* **2013**, *25* (16), 3373−3382.
(65) Frost, H.; Snurr, R. Q. Design Requirements for Metal-Organic Frameworks as Hydrogen Storage Materials. *J. Phys. Chem. C* **2007**, *111* (50), 18794−18803.
(66) Frenkel, D.; Smit, B. *Understanding Molecular Simulation: From Algorithms to Applications*; Academic Press: San Diego, 2002.
(67) Bae, Y.-S.; Snurr, R. Q. Molecular Simulations of Very High Pressure Hydrogen Storage Using Metal−Organic Frameworks. *Microporous Mesoporous Mater.* **2010**, *135* (1−3), 178−186.
(68) Kim, J.; Smit, B. Efficient Monte Carlo Simulations of Gas Molecules inside Porous Materials. *J. Chem. Theory Comput.* **2012**, *8* (7), 2336−2343.
(69) Buch, V. Path Integral Simulations of Mixed Para-D2 and Ortho-D2 Clusters: The Orientational Effects. *J. Chem. Phys.* **1994**, *100* (10), 7610−7629.
(70) Liu, J.; Rankin, R. B.; Karl Johnson, J. The Importance of Charge−Quadrupole Interactions for H2 Adsorption and Diffusion in Cubtc. *Mol. Simul.* **2009**, *35* (1−2), 60−69.
(71) Rappe, A. K.; Casewit, C. J.; Colwell, K. S.; Goddard, W. A.; Skiff, W. M. Uff, a Full Periodic-Table Force-Field for Molecular Mechanics and Molecular-Dynamics Simulations. *J. Am. Chem. Soc.* **1992**, *114* (25), 10024−10035.
(72) Basdogan, Y.; Keskin, S. Simulation and Modelling of Mofs for Hydrogen Storage. *CrystEngComm* **2015**, *17* (2), 261−275.
(73) Deeg, K. S.; Gutiérrez-Sevillano, J. J.; Bueno-Pérez, R.; Parra, J. B.; Ania, C. O.; Doblaré, M.; Calero, S. Insights on the Molecular Mechanisms of Hydrogen Adsorption in Zeolites. *J. Phys. Chem. C* **2013**, *117* (27), 14374−14380.
(74) Le, T. C.; Winkler, D. A. Discovery and Optimization of Materials Using Evolutionary Approaches. *Chem. Rev.* **2016**, *116* (10), 6107−6132.
(75) Haranczyk, M.; Rycroft, C. H.; Martin, R. L.; Willems, T. F. *Zeo++: High-Throughput Analysis of Crystalline Porous Materials 0.1.0*; Lawrence Berkeley National Laboratoy: Berkeley, 2012.
(76) Willems, T. F.; Rycroft, C. H.; Kazi, M.; Meza, J. C.; Haranczyk, M. Algorithms and Tools for High-Throughput Geometry-Based Analysis of Crystalline Porous Materials. *Microporous Mesoporous Mater.* **2012**, *149* (1), 134−141.
(77) Martin, R. L.; Willems, T. F.; Lin, L.-C.; Kim, J.; Swisher, J. A.; Smit, B.; Haranczyk, M. Similarity-Driven Discovery of Zeolite Materials for Adsorption-Based Separations. *ChemPhysChem* **2012**, *13* (16), 3595−3597.
(78) Frost, H.; Duren, T.; Snurr, R. Q. Effects of Surface Area, Free Volume, and Heat of Adsorption on Hydrogen Uptake in Metal-Organic Frameworks. *J. Phys. Chem. B* **2006**, *110* (19), 9565−9570.
(79) Simon, C. M.; Kim, J.; Lin, L.-C.; Martin, R. L.; Haranczyk, M.; Smit, B. Optimizing Nanoporous Materials for Gas Storage. *Phys. Chem. Chem. Phys.* **2014**, *16*, 5499−5513.
(80) Thornton, A.; Nairn, K.; Hill, J.; Hill, A.; Hill, M. Metal-Organic Frameworks Impregnated with Magnesium-Decorated Fullerenes for

DOI: 10.1021/acs.chemmater.6b04933
Chem. Mater. 2017, 29, 2844−2854

Methane and Hydrogen Storage. *J. Am. Chem. Soc.* **2009**, *131* (30), 10662−10669.
(81) Furukawa, H.; Ko, N.; Go, Y. B.; Aratani, N.; Choi, S. B.; Choi, E.; Yazaydin, A. O.; Snurr, R. Q.; O'Keeffe, M.; Kim, J.; Yaghi, O. M. Ultrahigh Porosity in Metal-Organic Frameworks. *Science* **2010**, *329* (5990), 424−428.
(82) Ibarra, I. A.; Yang, S.; Lin, X.; Blake, A. J.; Rizkallah, P. J.; Nowell, H.; Allan, D. R.; Champness, N. R.; Hubberstey, P.; Schroder, M. Highly Porous and Robust Scandium-Based Metal-Organic Frameworks for Hydrogen Storage. *Chem. Commun.* **2011**, *47* (29), 8304−8306.
(83) Yuan, D.; Zhao, D.; Sun, D.; Zhou, H.-C. An Isoreticular Series of Metal−Organic Frameworks with Dendritic Hexacarboxylate Ligands and Exceptionally High Gas-Uptake Capacity. *Angew. Chem., Int. Ed.* **2010**, *49* (31), 5357−5361.
(84) Park, K. S.; Ni, Z.; Cote, A. P.; Choi, J. Y.; Huang, R.; Uribe-Romo, F. J.; Chae, H. K.; O'Keeffe, M.; Yaghi, O. M. Exceptional Chemical and Thermal Stability of Zeolitic Imidazolate Frameworks. *Proc. Natl. Acad. Sci. U. S. A.* **2006**, *103* (27), 10186−10191.
(85) Fairen-Jimenez, D.; Moggach, S. A.; Wharmby, M. T.; Wright, P. A.; Parsons, S.; Duren, T. Opening the Gate: Framework Flexibility in Zif-8 Explored by Experiments and Simulations. *J. Am. Chem. Soc.* **2011**, *133* (23), 8900−8902.
(86) Abrahams, B. F.; Hoskins, B. F.; Liu, J.; Robson, R. The Archetype for a New Class of Simple Extended 3d Honeycomb Frameworks. The Synthesis and X-Ray Crystal Structures of Cd(Cn)5/3(Oh)1/3.1/3(C6h12n4), Cd(Cn)2.1/3(C6h12n4), and Cd(Cn)2.2/3h2o.Tbuoh (C6h12n4 = Hexamethylenetetramine) Revealing Two Topologically Equivalent but Geometrically Different Frameworks. *J. Am. Chem. Soc.* **1991**, *113* (8), 3045−3051.
(87) Andrés, R.; Brissard, M.; Gruselle, M.; Train, C.; Vaissermann, J.; Malézieux, B.; Jamet, J.-P.; Verdaguer, M. Rational Design of Three-Dimensional (3d) Optically Active Molecule-Based Magnets: Synthesis, Structure, Optical and Magnetic Properties of {[Ru(Bpy)3]2+, Clo4-, [Mniiicriii(Ox)3]-}N and {[Ru(Bpy)2ppy]+, [Miicriii(Ox)3]-}N, with Mii = Mnii, Niii. X-Ray Structure of {[Δru(Bpy)3]2+, Clo4-, [Δmniiδcriii(Ox)3]-}N and {[Λru(Bpy)2ppy]+, [Λmniiλcriii(Ox)3]-}N. *Inorg. Chem.* **2001**, *40* (18), 4633−4640.
(88) Lyndon, R.; Konstas, K.; Ladewig, B. P.; Southon, P. D.; Kepert, P. C. J.; Hill, M. R. Dynamic Photo-Switching in Metal−Organic Frameworks as a Route to Low-Energy Carbon Dioxide Capture and Release. *Angew. Chem., Int. Ed.* **2013**, *52* (13), 3695−3698.
(89) Li, H.; Sadiq, M. M.; Suzuki, K.; Ricco, R.; Doblin, C.; Hill, A. J.; Lim, S.; Falcaro, P.; Hill, M. R. Magnetic Metal−Organic Frameworks for Efficient Carbon Dioxide Capture and Remote Trigger Release. *Adv. Mater.* **2016**, *28* (9), 1839−1844.
(90) McDonald, T. M.; Mason, J. A.; Kong, X.; Bloch, E. D.; Gygi, D.; Dani, A.; Crocella, V.; Giordanino, F.; Odoh, S. O.; Drisdell, W. S.; Vlaisavljevich, B.; Dzubak, A. L.; Poloni, R.; Schnell, S. K.; Planas, N.; Lee, K.; Pascal, T.; Wan, L. F.; Prendergast, D.; Neaton, J. B.; Smit, B.; Kortright, J. B.; Gagliardi, L.; Bordiga, S.; Reimer, J. A.; Long, J. R. Cooperative Insertion of Co2 in Diamine-Appended Metal-Organic Frameworks. *Nature* **2015**, *519*, 303−308.
(91) Burtch, N. C.; Jasuja, H.; Walton, K. S. Water Stability and Adsorption in Metal−Organic Frameworks. *Chem. Rev.* **2014**, *114* (20), 10575−10612.
(92) Bouëssel du Bourg, L.; Ortiz, A. U.; Boutin, A.; Coudert, F.-X. Thermal and Mechanical Stability of Zeolitic Imidazolate Frameworks Polymorphs. *APL Mater.* **2014**, *2* (12), 124110.
(93) Bosch, M.; Zhang, M.; Zhou, H.-C. Increasing the Stability of Metal-Organic Frameworks. *Adv. Chem.* **2014**, *2014*, 182327.
(94) Coudert, F.-X. Systematic Investigation of the Mechanical Properties of Pure Silica Zeolites: Stiffness, Anisotropy, and Negative Linear Compressibility. *Phys. Chem. Chem. Phys.* **2013**, *15* (38), 16012−16018.
(95) DeSantis, D.; Mason, J. A.; James, B. D.; Houchins, C.; Long, J. R.; Veenstra, M. Techno-Economic Analysis of Metal−Organic Frameworks for Hydrogen and Natural Gas Storage. *Energy Fuels* **2017**, *31* (2), 2024−2032.
(96) James, B. D. *Hydrogen Storage Cost Analysis, Preliminary Results*; Project Id St100; U.S. Department of Energy: 2012. https://www.hydrogen.energy.gov/pdfs/review12/st100_james_2012_o.pdf.

DOI: 10.1021/acs.chemmater.6b04933
Chem. Mater. 2017, 29, 2844−2854